A NEW NON ISOLATED HIGH POWER FACTOR BATTERY CHARGER USING A QUADRATIC BUCK CONVERTER AS DC/DC STAGE

Marques Jr. O. N.; Praça, P. P.; Barreto, L. H. S. C.
Universidade Federal do Ceará
Departamento de Engenharia Elétrica
Caixa Postal 6001 – Campus do Pici
60.455-760 – Fortaleza – CE – Brazil
Phone: +55 85 4008-9581 / Fax: +55 85 4008-9574
Email: lbarreto@dee.ufc.br

***Abstract* - This work reports the operation and development of a high power factor battery charger which operates at high switching frequency. An optimum power factor correction is obtained using an ac–dc boost converter associated to a non dissipative snubber as a pre-regulator circuit, which presents reduced commutation losses. The same non dissipative snubber is associated to a quadratic Buck converter and then used as a dc–dc stage. The proposed system presents high power factor, high efficiency, low harmonic content, and good regulation.**

***Keywords* - Battery Charger, Boost PFC , Quadratic Buck**

I. INTRODUCTION

In the last few years, power factor correction, minimization of harmonic content and electromagnetic interference (EMI) levels, as well as reduction of size, weight and cost of battery charger has become the main concern of industry and academic researchers, as they present output dc voltage levels, constant switching frequency, reduced size and weight if compared to linear power supplies.

However, the input stages of battery charger are potential harmonic sources. Recently, there has been great interest about the reduction of input current harmonic content and power factor correction (PFC). Moreover, in many single phase applications the power levels can reach several kilowatts and, in some cases, the input voltage can be quite high as well. For such types of application, the conventional Boost PFC converter has been intensively used due to its intrinsic characteristics of dc-voltage gain, lower inductor volume and weight, and losses on the power devices, which will affect converter cost, efficiency, and power density [1] and [2]. An adequate modulation technique is necessary so that high power factor and low harmonic distortion can be achieved, as this work employs the Bang-Bang hysteresis current waveshaping control technique [3], [4], [5] for this purpose

Moreover, the Boost converter presents commutation and conduction losses, implying the reduction of efficiency. Conventional resonant and quasiresonant converters [6] and [7] provide zero-current switching (ZCS) and/or zero-voltage switching (ZVS) [8] and [9]. Such converters can operate at high frequencies, although they present load limitation (due to current and/or voltage peaks over the switches) and a specific frequency range as the design of filters becomes complex. A satisfactory alternative to achieve high frequency and high-power operation lies in the use of non dissipative snubbers [10].

The quadratic converter [11] provides a significantly wide conversion range for high frequency applications. The proposed battery charger employs a dc–dc quadratic Buck converter using a non dissipative snubber to achieve such optimum performance, as it is suitable to the required power level and provides soft switching a wide load range, as the conduction losses are almost the same as those observed in the hard-switched PWM converter.

This paper presents a battery charger composed by a PFC Boost converter and a quadratic Buck converter, using resonant cells to reduce commutation losses as shown in Fig. 1. The use of these two converters together as a battery charger is the main innovation of this work.

II. PROPOSED BATTERY CHARGER

The ac–dc and dc–dc nondissipative converters are shown in figs. 2 and 3, which operate with reduced commutation losses. In the proposed battery charger, main switches S_1

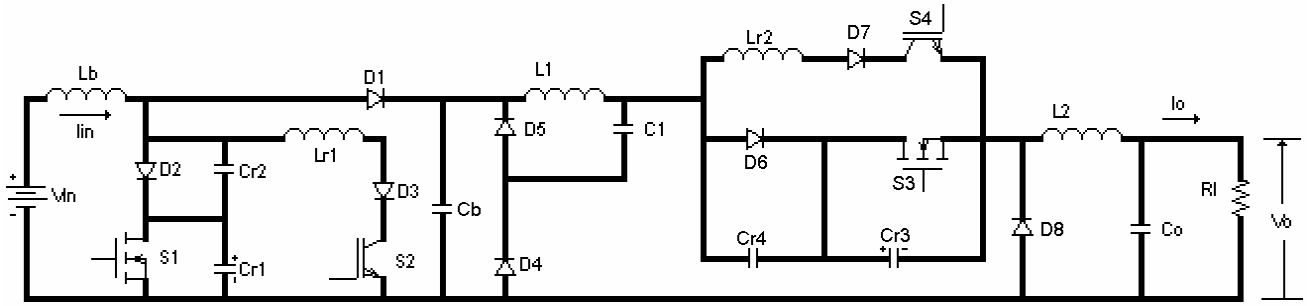

Fig. 1. Complete battery charger.

(Boost) and S_3 (Buck) are commutated in a ZVS way, and auxiliary switches S_2 (Boost) and S_4 (Buck) are commutated in a ZCS way due to the resonant cell, composed of resonant inductors (L_{r1} and Lr2) and resonant capacitors (C_{r1} ,C_{r2} ,Cr3 and C_{r4}). In order to simplify the analysis, the converters are analyzed apart.

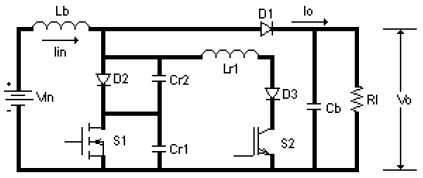

Fig. 2. Proposed PFC Boost converter.

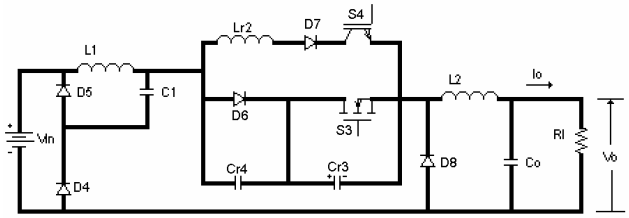

Fig. 3. Proposed quadratic Buck converter.

III. PRINCIPLE OF OPERATION OF THE AC–DC BOOST CONVERTER

A complete theoretical analysis for the approach shown in Fig. 2 is presented as follows. Since both converters present the same principle of operation, a single Boost converter will be analyzed. The analysis begins with the description of seven operation stages that determine a complete switching cycle.

First Stage (to, t1) (Fig. 4) - This stage begins when switch S2 is turned on in a ZCS way. During this stage the resonant inductor current (iLr) rises linearly from zero to the input current (Iin), causing D1 to turn off in a ZCS way. This stage finish when iLr = Iin.

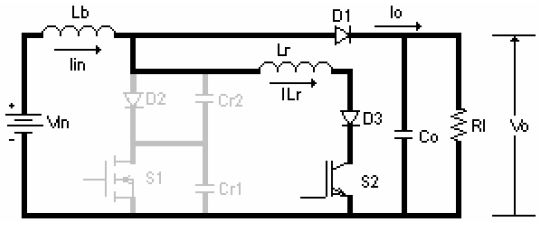

Fig. 4. First Stage (t_o, t_1).

Second Stage (t_1, t_2) (Fig. 5) - When the resonant inductor current (iLr) is equal to the input current (Iin), this stage begins. During this stage the resonance between the resonant capacitors (Cr1 and Cr2) and the resonant inductor (Lr), begins. In this stage the resonant capacitor 1 is discharged and the resonant capacitor 2 (Cr2) is charged. This stage finishes when resonant capacitor 1 (Cr1) is completely discharged.

Third Stage (t_2, t_3) – (Fig. 6). This stage begins when the voltage on the resonant capacitor 1 (Cr1) is equal to zero. During this stage the resonant capacitor 2 (Cr2) is in resonance with the resonant inductor (Lr), alone. When the resonant inductor current is equal to zero this stage finishes. After the resonant inductor current reaches zero the switch S2 can be turned off in a ZCS way. During this stage the main switch S1 is turned on in a ZVS way.

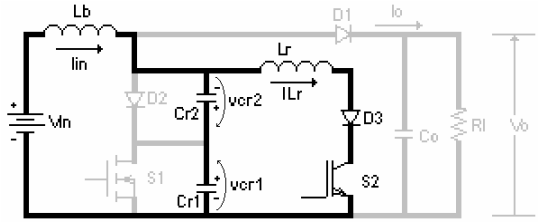

Fig. 5. Second Stage (t_1, t_2).

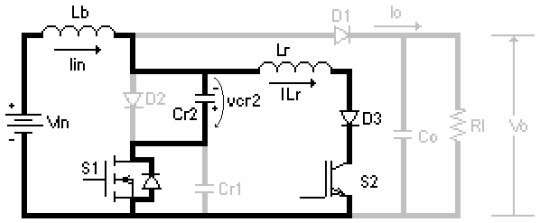

Fig. 6. Third Stage (t_2, t_3).

Fourth Stage (t_3, t_4) – (Fig. 7). This stage begins when iLr is equal to zero, and it finishes when the voltage on resonant capacitor 2 (Cr2) is zero. During this stage the resonant capacitor 2 (Cr2) is discharged in a linear way by the input current (Iin).

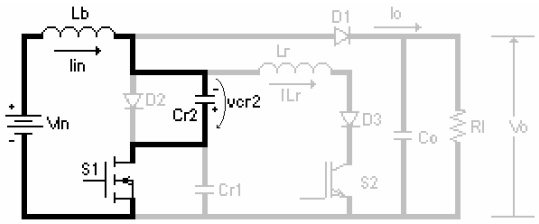

Fig. 7. Fourth Stage (t_3, t_4).

Fifth Stage (t_4, t_5) – (Fig. 8). This stage begins when the voltage on resonant capacitor 2 (Cr2) is equal to zero, turning on diode D2 in a ZVS way. During this stage the energy is stored in the Boost inductor (Lb). When switch S1 is turned off in a ZVS way this stage finishes.

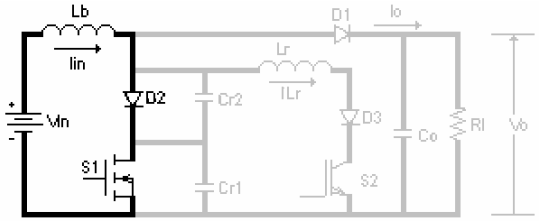

Fig. 8. Fifth Stage (t_4, t_5).

Sixth Stage (t_5, t_6) – (Fig. 9). When the main switch S1 is turned off in a ZVS way, this stage begins. The input current pass through the resonant capacitor 1 (Cr1), this capacitor is charged up to the output voltage (V0). This stage finishes when diode D1 is turned on in ZVS way.

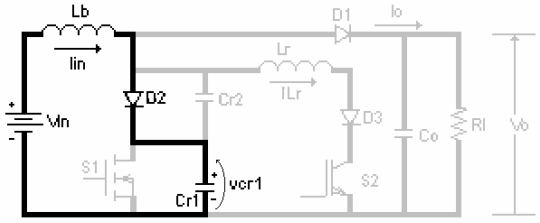

Fig. 9. Sixth Stage (t_5, t_6).

Seventh Stage (t_6, t_7) – (Fig. 10). During this stage the energy stored in the Boost inductor (Lb) feeds the load. This stage finish when it begins the next switching cycle.

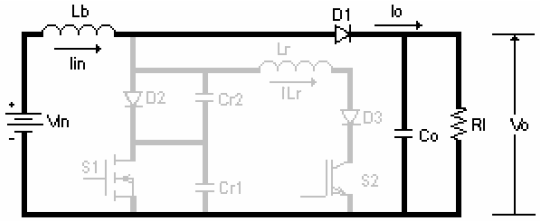

Fig. 10. Seventh Stage (t_6, t_7).

The transference function between V_0 and V_{in} is given by:

$$G = \frac{V_o}{V_{in}} = \frac{1}{1-\left\{D+\frac{K_1}{2p}\left[\arccos\left(-\frac{1}{X}\right)+\frac{X+1}{Xa}+\frac{a}{2}\right]\right\}} \quad (1)$$

Where:

$$a = \frac{I_{in}}{V_0}\sqrt{\frac{L_{r1}}{C_r}} \quad (2)$$

$$K_1 = \frac{f_s}{f_o} \quad (3)$$

f_s = switching frequency;
f_0 = resonant frequency;
D = duty cycle Boost converter;
X = ratio between Cr1 and Cr2.

From the operating stages described above, one can obtain the waveforms shown in Fig. 11.

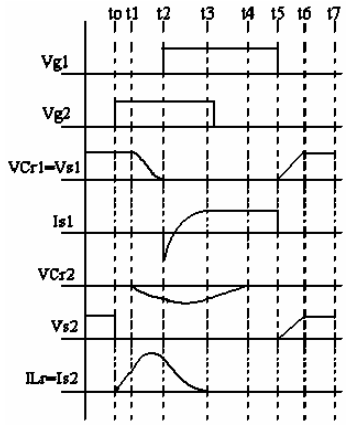

Fig. 11. Boost converter theoretical waveforms.

IV. PRINCIPLE OF OPERATION OF THE DC–DC QUADRATIC BUCK CONVERTER

Fig. 3 shows the quadratic Buck converter associated to a nondissipative snubber employed as a dc–dc stage. From the operating stages, which are basically the same as those of the Boost converter, one can obtain the waveforms shown in Fig. 12.

The transference function between V_0' and V_{in}' is given by:

$$G' = \frac{V_o'}{V_{in}'} = \left\{1-\left\{D'+\frac{K_1'}{2p}\left[\arccos\left(-\frac{1}{X'}\right)+ \right.\right.\right. \quad (4)$$
$$\left.\left.\left. +\frac{(X'+1)(1+D'))}{X'a'}+\frac{a'}{2(1+D')}\right]\right\}\right\}^2$$

Where:
f_s´ = switching frequency;
f_0´ = resonant frequency;
D´ = duty cycle;
X´ = ratio between Cr3 and Cr4.

$$a' = \frac{I_{in}'}{V_0'}\sqrt{\frac{L_{r2}}{C_r}} \quad (5)$$

$$K_1' = \frac{f_S'}{f_0'} \quad (6)$$

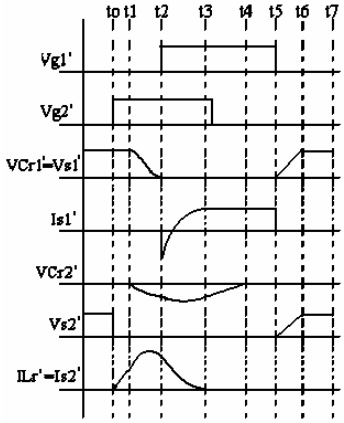

Fig. 12. Quadratic Buck converter theoretical waveforms

V. CONTROL STRATEGY

The block diagram of the digital control circuit is shown in Fig. 13. This converter operates with constant switching frequency and high power factor, using a Bang-Bang current control strategy. The use the bang-bang hysteresis current waveshaping control technique applied in the Boost converter in order to achieve a quasi unity power factor. With the Buck converter was used a digital control to maintain output voltage constant.

The input current and line voltage samples are obtained from Rshu and Rt1 / Rt2 sensors. The voltage sample is rectified in the Accuracy Rectifier block.

The Signal Conditioning Circuit was a filter. The controller is implemented to provide the control signal (Vc), which is multiplied by Vinref. Then this signal is added to

the sawtooth signal generating the reference current signal (Iref). This operation is made inside of PIC (16c73a).

The drive signals are obtained by comparing the current feedback signal, generated in the sensor Rshu, with the reference current signal (Iref).

The signal obtained from the comparator block output drives auxiliary switch S2 directly. The same signal will drive switch S1, but only when the zero voltage transition on the switch is satisfied.

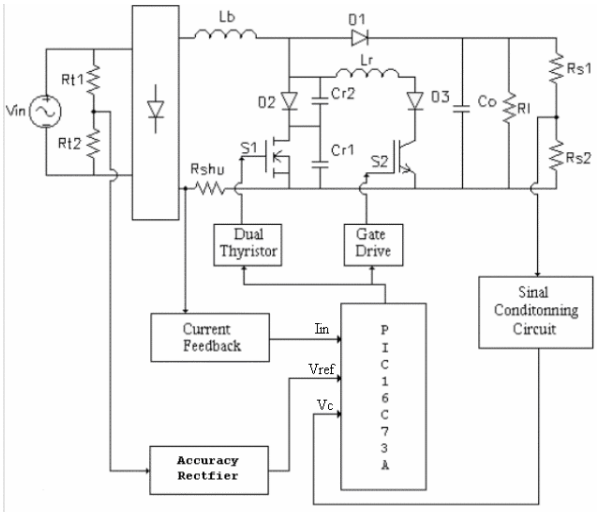

Fig. 13. Boost Converter associated to a non-dissipative snubber and the digital control circuit.

The algorithm that applies the hysteresis "bang-bang" control strategy follows the flow chart shown in Fig. 14. The called stage of "Start" is characterized by the declaration of variables. In the stage called "Read Vin", happens the reading of the A/D channel corresponding to the input voltage. In the stage called "Read Iin", happens the reading of the A/D channel corresponding to the input current. However, the conversion time is very sluggish (16us each) then the reload of the output voltage was not used.

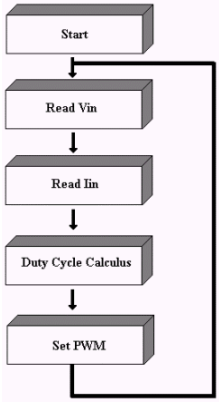

Fig. 14. Flow chart representation of the employed algorithm.

VI. SIMULATION AND EXPERIMENTAL RESULTS

The battery charger proposed in this paper (Fig. 1) has been intensively studied via simulation using PSpice software, where the following parameter set is employed:

S1 = IRFP460; S2, S4 = IRGBC20F; S3 = IRFP460;
Dx = ideal; Lr1 = 2.5 uH; Lr2 = 2.5 uH;
Lb = 500 uH; L1 = 200 uH; L2 = 20 uH;
Cr1 = 10nF; Cr2 = 27 nF; Cr3 = 7.5 nF;
Cr4 = 27 nF; C1 = C0 = 10uF; Cb = 100 uF;
Vin = ~110V; Vo = 27 V; fs = 100 KHz;
Po = 300 W.

A battery charger was built using the following parameter set. The differences of values among some components of prototype and of simulation are for the fastest simulation.

S1 = IRFP460; S2, S4 = IRGBC20F; S3 = IRFP460;
Dx = MUR1560; Lr1 = 2.5 uH; Lr2 = 2.5 uH;
Lb = 500 uH; L1 = 500 uH; L2 = 50 uH;
Cr1 = 10nF; Cr2 = 27 nF; Cr3 = 7.5 nF;
Cr4 = 27 nF; C1 = C0 = 100uF; Cb = 680 uF;
Vin = ~110V; Vo = 27 V; fs = 100 KHz;
Po = 300 W.

Fig. 15 shows the simulation and experimental results for power factor measurements. The power factor calculated for this prototype reached 0.990.

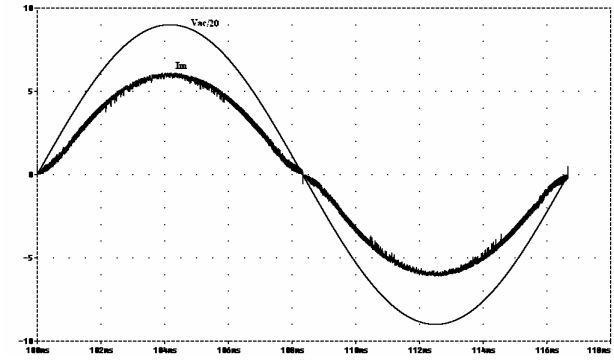

(a)

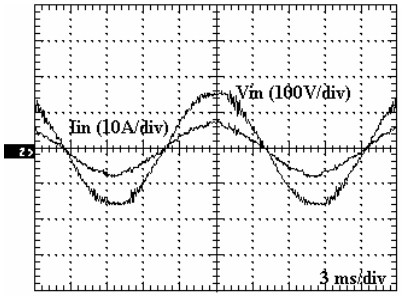

(b)

Fig. 15. Input Voltage and Current:
a) Simulation;
b) Experimental.

Figs. 16 and 17 show the commutation in the active switches. It can be seen that the main switches do not present current and/or voltage stresses, as well as the commutations are non dissipative, and the auxiliary switches commutate in a ZCS way. These waveforms are similar to that obtained in theoretical analyzes of the converters.

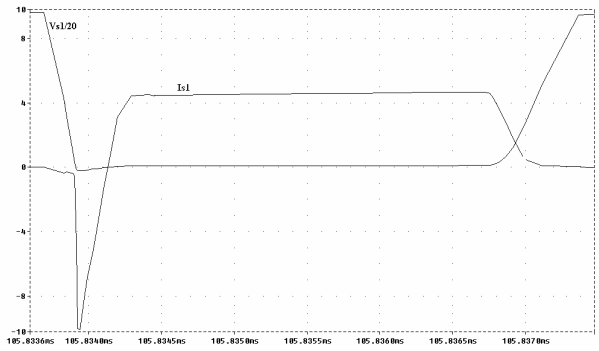

(a)

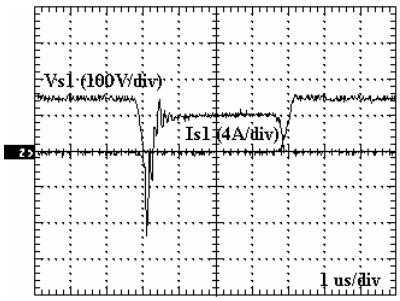

(b)

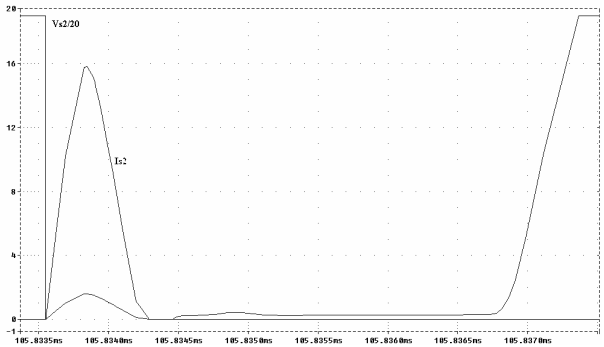

(c)

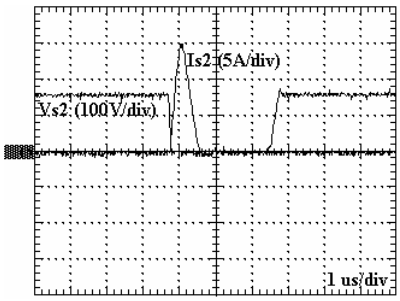

(d)

Fig. 16 Active switches in boost converter:
(a) Main switch S1 waveforms concerning simulated results;
(b) Main switch S1 waveforms concerning Experimental results;
(c) Auxiliary switch S2 waveforms concerning simulated results;
(d) Auxiliary switch S2 waveforms concerning experimental results

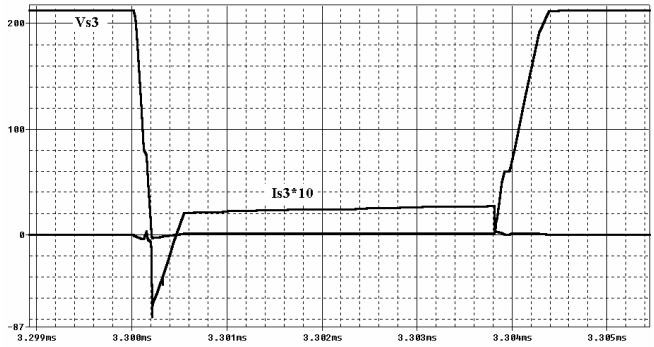

(a)

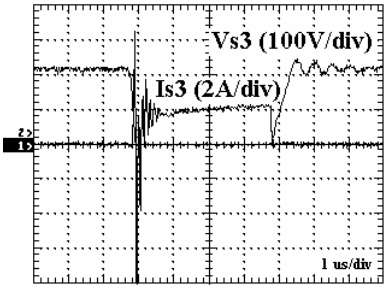

(b)

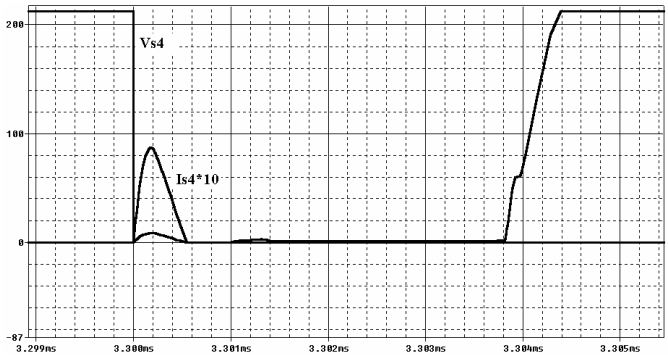

(c)

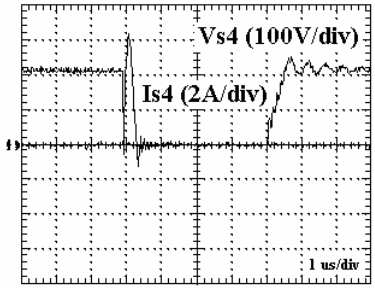

(d)

Fig. 17 Active switches in quadratic Buck converter:
(a) Main switch S3 waveforms concerning simulated results;
(b) Main switch S3 waveforms concerning Experimental results;
(c) Auxiliary switch S4 waveforms concerning simulated results;
(d) Auxiliary switch S4 waveforms concerning experimental results.

Fig. 18 shows the quadratic Buck converter voltages. It can be seen a significantly wide conversion range.

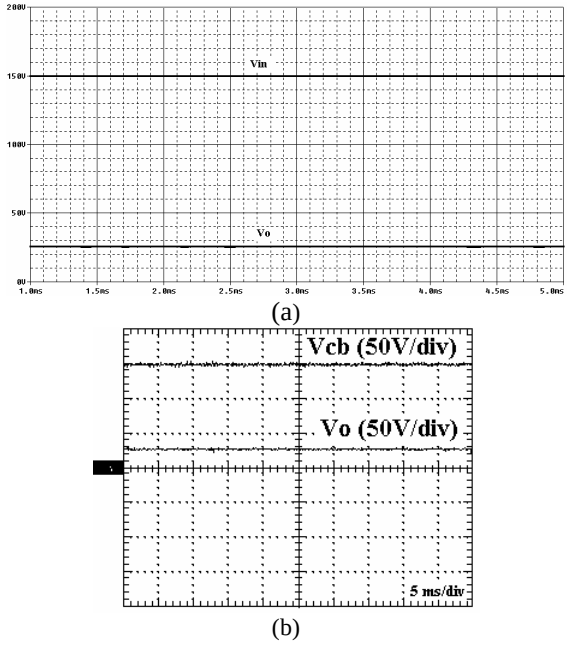

(a)

(b)

Fig. 18. Quadratic Buck converter voltages:
a) Simulation;
b) Experimental.

Current and voltage total harmonic distortion rates (Fig. 19), where the current THD was obtained, in the simulation and in the experimentation, and the voltage THD obtained only in the prototype. In the simulation, the current THD value is equal to 4.85%, and in the prototype the current and voltage THD values are 2.84% and 2.83%, respectively. In this figure the fundamental was omitted to facilitate the visualization.

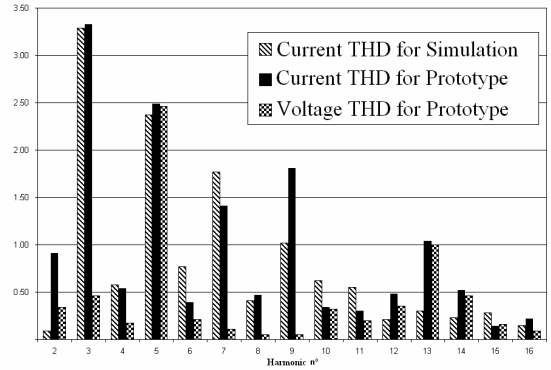

Fig. 19. Current and voltage total harmonic distortion rates.

VII. CONCLUSION

This paper reports the analytical, simulation and experimental developments of a battery charger using the PFC ac–dc Boost associated to a non dissipative snubber. It has been demonstrated that the use of control technique in combination with the non dissipative snubber implies a highly efficient power factor correction pre-regulator circuit with reduced commutation losses. The proposed battery charger employs a quadratic Buck converter as a dc–dc converter, which operates with soft commutation by using a non dissipative snubber. These converters work in a soft switching way, the main switch (S1 and S3) commutates in a ZVS way and the auxiliary switch (S2 and S4) commutates in a ZCS way. Simulation results confirm the non dissipative switching of both switches.

The prototype presents high power factor (0.990), low voltage and current harmonic distortion (2.83% and 2.84% respectively) and good regulation (Fig. 18). The initial proposal then was attended thoroughly.

ACKNOWLEDGMENTS

The authors thank Thorton Inpec, Siemens, Texas Instruments, CAPES, CNPQ and FUNCAP by the support.

REFERENCES

[1] M. T. Zhang, Y. Jiang, F. Lee, C. Joavanovic, and M. Milam, “Singlephase three-level boost power factor correction converter,” in Proc. IEEE APEC, 1995, pp. 434–439.

[2] B. A. Miwa, D. M. Otten, and M. F. Schlecht, “High efficiency power factor corretion using interleaving techniques,” in Proc. IEEE APEC, 1992, pp. 368–375.

[3] R. Tóffano Jr, C. H. G. Treviso, V. J. Farias, J. B. Vieira Jr, and L. C. de Freitas, “A self-resonant-PWM boost converter with unity power factor operation by using bang-bang current control strategy with fixed switching frequency,” in Proc. EPE, 1997, pp. 4.454–4.457.

[4] M. Kazerani, G. Joos, and P. D. Ziogas, “A novel active current waveshaping technique for solid state input power factor conditioners,” in Proc. IEEE IECON, 1989, pp. 99–105.

[5] K. Fung, W. Ki, and K. T. M. Philip, “Analysis and measurement of DCM power factor correctors,” in Proc. IEEE PESC, 1999.

[6] F. C. Lee, “High-Frequency quasiresonant converter technologies,” Proc. IEEE, vol. 76, pp. 377–390, Apr. 1988.

[7] I. Barbi, J. C. Bolacell, and J. B. Vieira, Jr, “A forward pulse-width modulated quasiresonant converter: Analysis, design and experimental results,” in Proc. IEEE IECON, 1989, pp. 21–26.

[8] F. C. Lee, G. Hua, and C. S. Leu, “Novel zero-voltage-transition PWM converters,” in Proc. IEEE PESC, 1992, pp. 55–61.

[9] V. J. de Freitas, P. S. Farias, J. B. Vieira Jr, H. L. Hey, and D. F. Cruz, “An optimum ZVS-PWM dc-to-dc converter family: Analysis, simulation and experimental results,” in Proc. IEEE PESC, 1992, pp. 229–235.

[10] L. H. S. C. Barreto, A. A. Pereira, V. J. Farias, L. C. de Freitas, and J. B. Vieria Jr, “A boost converter associated with a new nondissipative snubber,” in Proc. IEEE APEC, 1998, pp. 1077–1083.

[11] Maksiomovic, D. and Cuk S., ”Switching Converters with Wide DC conversion Range.”, IEEE Transaction on Power Electronics Vol. 6 no 1, Record pp. 151-157. Jan/91.